



Experimental Research of Two-phase Rotating Detonation Combustor Operating with High Total Temperature Air

G. Ge¹, Y. Ma², Z. Xia¹, H. Ma^{1†}, L. Deng³ and C. Zhou¹

¹ School of Mechanical Engineering, Nanjing University of Science and Technology, Nanjing, Jiangsu, 210094, China

² Department of Aeronautical Mechanical Engineering and Command, Qingdao Campus of Naval University of Aeronautics and Astronautics, Qingdao, Shandong, 266100, China

³ Institute of Chemical Materials, China Academy of Engineering Physics, Mianyang, Sichuan, 621999, China

†Corresponding Author Email: mahuokok@163.com

(Received November 26, 2021; accepted April 24, 2022)

ABSTRACT

Experiments on a two-phase rotating detonation combustor operating with gasoline and high total temperature air were conducted to investigate the initiation characteristics, operation mode, and propagation characteristics of a two-phase rotating detonation wave (RDW). The outer diameter, inner diameter, and length of the annular combustor were 204 mm, 166 mm, and 155 mm, respectively. The initiation characteristics, operation mode, and propagation characteristics of the two-phase RDW were studied by varying the total air temperature. The experimental results show that the initiation time of the RDW first decreases and then increases with an increase in the total air temperature and reaches an extreme value at a total air temperature of 713 K. Four operation modes (failure, intermittent detonation, single wave, coexistence of double wave collision, and single wave) of the detonation combustor were found for different total air temperatures. The effect of the total air temperature on the peak pressure stability and propagation frequency of the RDW was studied in detail. From the results, the effect of the equivalence ratio on the working characteristics of a rotating detonation engine (RDE) was investigated at a total air temperature of 713 K. Four detonation propagation modes (sporadic detonation, intermittent detonation, single-wave mode, coexistence of double-wave collision and single wave) were obtained in the combustor. When the equivalence ratio was 0.52, the detonation initiation failed. The pressure characteristics in the combustor and propagation frequency of the RDW were studied with different equivalence ratios. In addition, a long-duration test was performed for 3 s to verify the continuous working feasibility of the two-phase RDE.

Keywords: Two-phase rotating detonation; Total air temperature; Initiation characteristics; Propagation characteristics; Equivalence ratio; Long-duration test.

1. INTRODUCTION

The rotating detonation engine is a novel propulsion concept that utilises one or multiple detonation waves propagating in an annular combustor to produce a steady thrust (Wolanski 2013). Owing to its compact structure, high operating frequency, high thermal cycle efficiency, and stable thrust, the RDE has the potential for use in future astronautic propulsion systems.

Significant investigations of RDEs fuelled by gaseous fuels have been conducted. These studies include: 1) the effects of the mass flow rate (Xie *et al.* 2018; Deng *et al.* 2017; Liu *et al.* 2015) and

equivalence ratio (Anand *et al.* 2016; Xia *et al.* 2019) on the wave speed performance (Rankin *et al.* 2017) of RDW; 2) the stability of rotating detonation wave under subsonic (Bykovskii and Vedernikov 2003) and supersonic injection (Frolov *et al.* 2015) of reactants; and 3) the ignition characteristics under different precombustion pressures (Fotia *et al.* 2018) and energy depositions (Yang *et al.* 2016; Peng *et al.* 2015). Researchers have revealed that the stability of the RDW and the operation map of the RDE are closely related to the injection configuration (Frolov *et al.* 2015). Moreover, the basic operating modes of the RDE are identified as steady single wave (Xia *et al.* 2019), coexistence of single wave and multiple waves (Ge *et al.* 2019), steady multiple waves (Liu *et al.* 2015), multiwave collisions (Rankin *et al.*

2017), and longitudinal pulsed detonation (Frolov *et al.* 2015).

With deeper research on RDE and the demand for engineering applications, many research institutions have focused more on studying two-phase rotating detonation engines operating with liquid fuels, which have higher density specific impulses than gaseous fuels.

In the research of two-phase RDE, Bykovskii has extensively investigated kerosene/oxygen enriched air (Bykovskii *et al.* 1997, 2006a), diesel/oxygen (Bykovskii *et al.* 2006b), kerosene/liquid oxygen, kerosene/oxygen, and gasoline/oxygen-enriched air (Bykovskii *et al.* 2014) as propellants. The effects of the mass flow rate (Zheng *et al.* 2015), equivalence ratio (Li *et al.* 2020), and oxygen mass fraction (Wang *et al.* 2017) on the wave speed performance and pressure characteristics of the RDW were studied experimentally. In addition, the thrust performance (Zheng *et al.* 2017), operation mode (Wang *et al.* 2017), ignition characteristics under different ignition energies and oxygen mass fractions (Kindracki 2014), and atomisation flow field (Kindracki 2012) were investigated. Bykovskii *et al.* (2016, 2019) studied the continuous detonation of aviation kerosene and air, with the addition of hydrogen or syngas, in an annular cylindrical combustor. Frolov *et al.* (2017) fed liquid propane into the hydrogen-air mixtures after the formation of continuous detonation combustion and obtained the continuous propagation of a two-phase rotating detonation wave. Kindracki (2015) performed rotating detonation combustion with kerosene, hydrogen, and air as propellants to study the influence of the hydrogen mass fraction in the fuel on the combustor pressure and detonation wave velocity.

Some researchers have used high-temperature air as an oxidant to study the propagation characteristics of RDW. Wang *et al.* (2015) first realised air-breathing rotating detonation fuelled by hydrogen at a total temperature of 860 K in a direct-connect

experimental facility. Frolov *et al.* (2018) performed a series of firing tests of a hydrogen-fuelled detonation ramjet model in a pulsed wind tunnel at an approach-airstream Mach number of 5.7 and a stagnation temperature of 1500 K. It was found that the operation mode of the combustor changed from rotating detonation to longitudinal pulse detonation with an increase in equivalence ratio. The maximum mean thrust and fuel-based specific impulse were 1550 N and 3300 s, respectively.

In previous research, the oxidant used in the study of two-phase rotating detonation was almost entirely oxygen-enriched air at atmospheric temperature. The chemical reactivity of gas-liquid propellants with normal-temperature air as an oxidant is relatively low, and it is difficult to inspire a continuous RDW in low-reactivity mixtures. Moreover, the effect of total air temperature on the propagation characteristics of rotating detonation waves has not attracted much attention. In this study, high total temperature air was utilised to accelerate the evaporation rate of gasoline droplets. Under the shear force of high total temperature air, gasoline droplets break up and evaporate rapidly to improve the mixing effect and chemical reactivity of propellants. Two-phase rotating detonation tests were performed under different total air temperatures and equivalence ratios. The initiation characteristics, operation modes, and propagation characteristics of the detonation wave were analysed in detail. In addition, a long-duration test was performed for 3 s to verify the continuous working feasibility of the two-phase RDE operating with high total temperature air and gasoline.

2. EXPERIMENTAL FACILITY AND MEASUREMENT METHODOLOGY

Figure 1 shows the two-phase RDE experimental facility, consisting of a model RDE combustor, gasoline and air delivery system, ignition system, heating system, control system, and data-acquisition system.

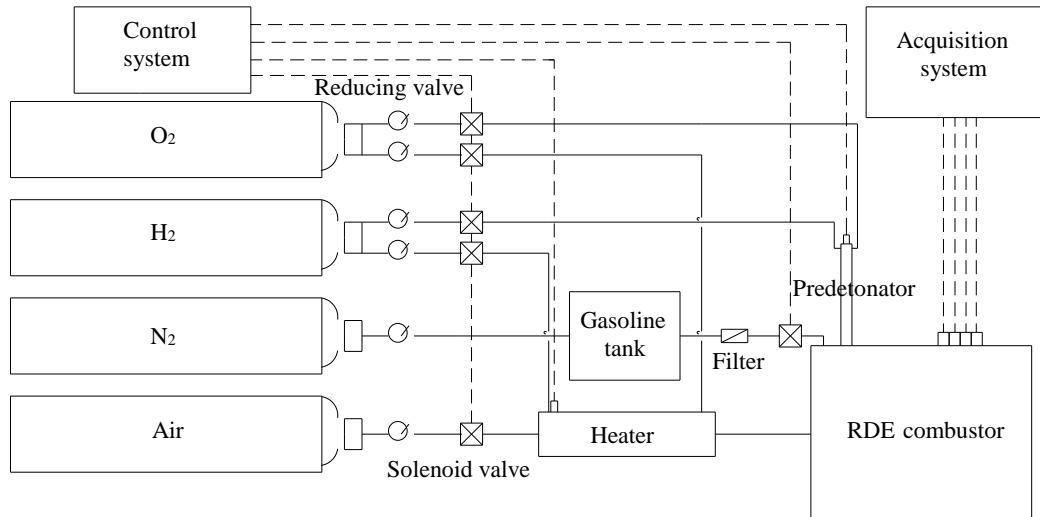


Fig. 1. Diagram of the two-phase RDE experimental facility.

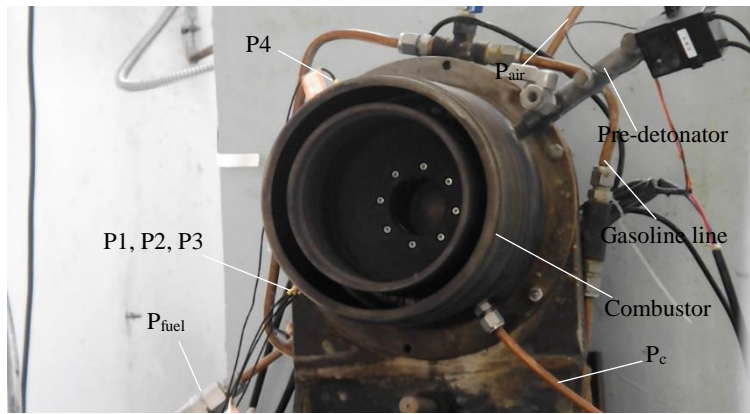


Fig. 2. Physical map of the two-phase rotating detonation combustor.

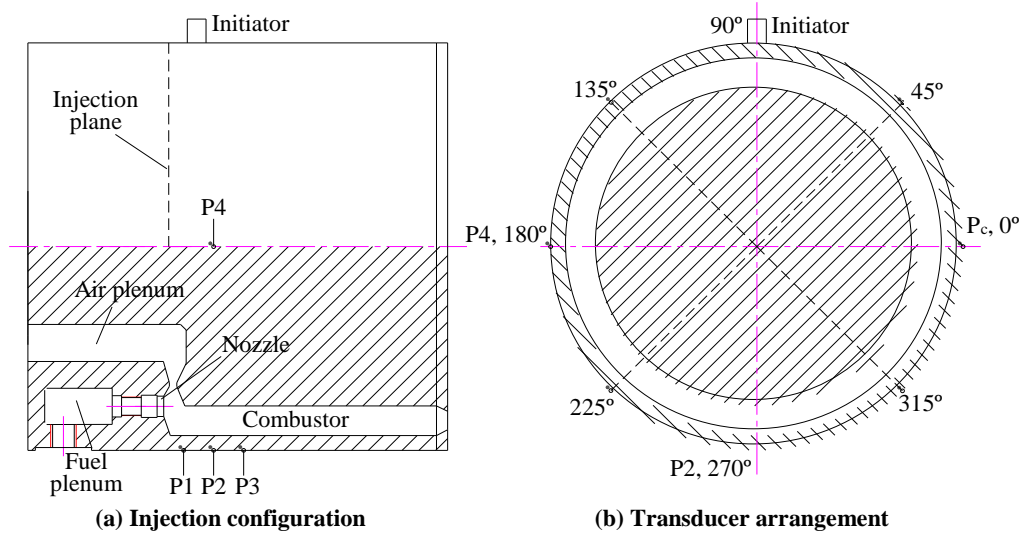
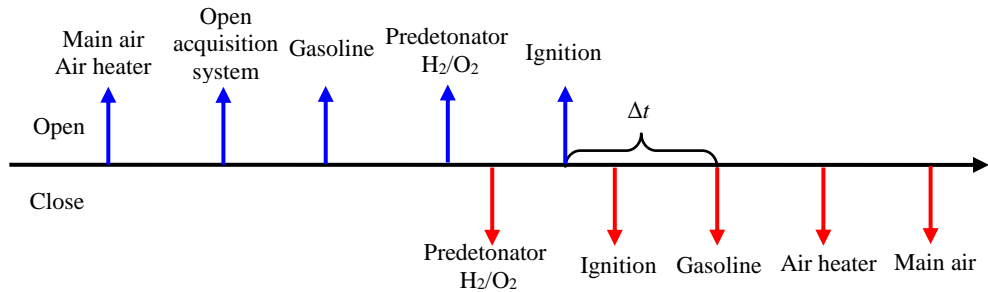


Fig. 3. Diagram of injection configuration and transducer arrangement.

Figure 2 shows a physical map of the two-phase rotating detonation combustor. The inner diameter, outer diameter, and length of the annular combustor were 166 mm, 204 mm, and 155 mm, respectively, resulting in a channel width of 19 mm. A slit-nozzle impingement model was applied to achieve high-quality mixing of gasoline and air, as shown in Fig. 3(a). An air heater with cold air-hydrogen as a propellant is used to heat the incoming air to a high total temperature. The oxygen mass fraction in the oxidant was maintained constant by adding oxygen to the air heater outlet. The high total temperature air enters the combustor through the Laval nozzle-like slit, whereas gasoline is injected through 36 uniformly distributed nozzles along the head of the combustor. The minimum size of atomised gasoline droplets can reach 20 μm in cold flow. The gasoline and air mass flow rates were measured upstream of the respective electromagnetic valves with a flow meter. The global equivalence ratios in all tests were calculated using the gasoline and oxygen mass flow rates. The detonation in the combustor was initiated using a vertically mounted pre-detonator, approximately 16 mm downstream of the injection plane. Hydrogen and oxygen were separately injected into the pre-detonator (20 mm diameter, 600

mm long). The mixtures were ignited by a spark when the static pressures in the gasoline and air plenums reached a steady state. The pre-detonator and combustor were separated by a thin plastic membrane, which was destroyed during each test, to minimise the interaction between the combustor and pre-detonator before ignition. The ambient temperature was 20 °C, and the backpressure at the combustor exit was 1 atm during the tests.

Time-dependent pressure signals in the detonation channel were applied to evaluate the operation mode and propagation characteristics of the detonation wave in the combustor. Piezoelectric pressure transducers were used to acquire the time-dependent dynamic pressure fluctuations in the combustor. The resonant frequency of this type of piezoelectric pressure transducer was greater than 100 kHz, and the rise time was less than 1 μs . Diffused silicon pressure transmitters measured the average static pressure in the plenums and combustor with a sensitivity of 0.5% FS. The piezoelectric pressure transducers and diffused silicon pressure transmitters were flush-mounted to reduce the interference to the detonation wavefront. The arrangement of the instruments is shown in Fig. 3. The piezoelectric

**Fig. 4. Schematic of experimental time sequence.**

pressure transducers P1, P2, and P3 were located 8 mm, 24 mm, and 40 mm downstream of the injection plane, respectively. P1, P2, and P3 were located at the same circumferential position. The diffused silicon pressure transmitter P_c was at the same axial position as P2 and P4, and the phase difference between them was 90°, as shown in Fig. 3(b). An NI X series multifunction DAQ with a data acquisition card (USB-4716) based on the NI-STC3 synchronisation technology was used to capture the pressure signals. The instruments were sampled at an acquisition rate of 250 kHz throughout the test.

Figure 4 shows the time sequence of the two-phase RDE tests. Data acquisition was triggered after the beginning of the main air and heating system. High total temperature air enters the annular combustor as an oxidant. The gasoline valve opens when the average pressure in the air plenum reaches a steady state, and the initiator valves subsequently open. The initiator sparks fires after a steady injection of gasoline. The detonation wave formed in the predetonator propagated into the combustor, and the RDE began to work in the detonation mode. Δt is the working time of the two-phase RDE. At the end of the tests, the gasoline injection and heating system stopped, and the flameout and cooling of the combustor were realised by the continuous injection of cold air for a period of time. Owing to the heavy heat loading and the impact of shock waves on the combustor and transducers, the test duration was set to 1 s.

3. RESULTS AND DISCUSSION

A series of two-phase rotating detonation firing tests were performed by varying the total air temperature and equivalence ratio. Table 1 lists the test conditions used in this study. The effects of total air temperature on the propagation characteristics and operation mode of the RDW were studied at an air mass flow rate of 1110.0 g/s, and gasoline mass flow rate of 85.7 g/s, resulting in an equivalence ratio of 1.19. When the total air temperature was 483 K, detonation initiation failed. When the total air temperature was increased to 573 K, the detonation wave was successfully initiated, and the propagation mode of the RDW was an intermittent detonation. When the total air temperature was between 643 K and 713 K, the propagation stability of the RDW was enhanced, and the detonation combustor operated in the single-wave mode. Upon further increase of the total air temperature to 793 K, the propagation mode of the RDW transformed from a single wave mode to the coexistence of double wave collision and single wave. With an increase in the total air temperature, the propagation frequency of the RDW first increased and then decreased, with the maximum value being approximately 713 K.

From the results from Case #1–5, the effect of the equivalence ratio on the combustor working characteristics was investigated at the air mass flow rate of 1110.0 g/s and total air temperature of 713 K.

Table 1 Experimental condition.

Case	Φ	T_0/K	$\dot{m}_{air}/(g/s)$	$\dot{m}_{fuel}/(g/s)$	f_d/Hz	Propagation mode
#1	1.19	483.0	1110.0	85.7	-	Failure
#2	1.19	573.0	1110.0	85.7	1672.4	Intermittent detonation
#3	1.19	643.0	1110.0	85.7	1782.2	Single wave
#4	1.19	713.0	1110.0	85.7	1900.9	Single wave
#5	1.19	793.0	1110.0	85.7	1835.5	Double wave collision/Single wave
#6	0.53	713.0	1110.0	38.4	-	Failure
#7	0.61	713.0	1110.0	44.2	1452.0	Sporadic detonation
#8	0.66	713.0	1110.0	47.9	1521.7	Intermittent detonation
#9	0.79	713.0	1110.0	57.3	1613.7	Double wave collision/Single wave
#10	0.84	713.0	1110.0	62.4	1818.2	Double wave collision/Single wave
#11	0.97	713.0	1110.0	70.3	1827.3	Double wave collision/Single wave
#12	1.06	713.0	1110.0	76.3	1849.1	Single wave
#13	1.25	713.0	1110.0	90.6	1878.4	Single wave
#14	0.84	713.0	1110.0	62.4	1922.3	Long-duration test

It was found that the continuous self-sustained propagation of the RDW was realised in the combustor during the equivalence ratio range 0.79–1.25. With an increase in the equivalence ratio, the propagation mode of the RDW transformed from the hybrid mode of double wave collision and single wave to the single wave mode. When the equivalence ratio was decreased to 0.61–0.66, the propagation stability of the RDW worsened, and the propagation mode transformed to intermittent detonation or sporadic detonation. When the equivalence ratio was further decreased to 0.52, the detonation initiation failed. In addition, with the increase in the equivalence ratio, the propagation frequency of the RDW first increased and then decreased, and the maximum value was obtained at an equivalence ratio of 1.19. Under this condition, the propagation frequency of the RDW was 1900.9 Hz, and the corresponding propagation velocity was approximately 1104.8 m/s. In Table 1, Φ is the equivalence ratio of the propellants, T_0 is the total air temperature, and \dot{m}_{air} and \dot{m}_{fuel} are the air and gasoline mass flow rates, respectively. F_d is the dominant frequency of the high-frequency pressure signals in the combustor, obtained from the fast Fourier transform. In this study, p_c is the time-averaged pressure in the combustor, and p_{air} and p_{fuel} are the time-averaged pressures in the air and gasoline plenums, respectively.

3.1 Effect of Total Air Temperature on Initiation Characteristics

In Case #1, the incoming air was heated to 483 K at an equivalence ratio of 1.19, as shown in Table 1. The initial detonation wave formed in the predetonator tube entered the combustor and failed to ignite the gasoline–air mixtures. However, under this condition, the evaporation rate of gasoline droplets is relatively low, and there is a large quantity of large-diameter gasoline droplets existing in the reactants, which require sufficient ignition energy for detonation initiation. Furthermore, the exit area of the predetonator tube is much smaller than that of the annular combustor. When the initial detonation wave propagated into the enlarged annular combustor, a significant expansion led to decoupling of the detonation wave.

Figure 5 shows the time-dependent pressure signals during the initiation stage of the RDW at a total air temperature of 713 K. It was found that P_4 and P_c detected the first pressure peak at approximately the same time, which indicates that the initial detonation wave from the predetonator decoupled and propagated in two opposite directions after entering the annular combustor. In this study, the time difference between the first pressure peak measured by P_c and P_2 is defined as the initiation time of the RDW. P_c detects the first pressure peak at approximately 3740.732 ms, and the peak pressure is approximately 0.61 MPa, which is close to the peak pressure of the detonation wave. Utilising the transducer arrangement shown in Fig. 3, the decoupled leading shock wave measured by P_c propagated clockwise. Two leading shock waves propagating in opposite directions collided for several cycles, and the weaker wave gradually

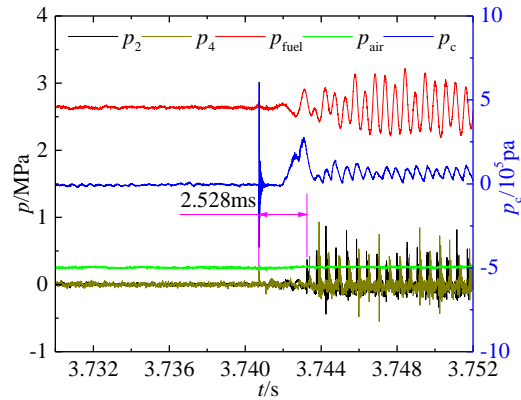


Fig. 5. Initiation stage of RDW in Case #4.

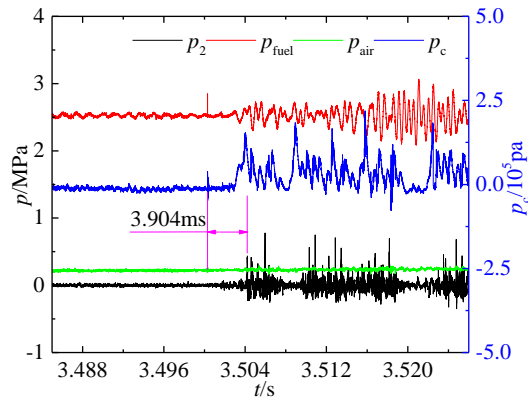


Fig. 6. Initiation stage of RDW in Case #2.

disappeared. After approximately 2.528 ms, combined with the effects of combustor curvature, propellant injection, and boundary layer development, the flame front accelerated and coupled with the leading shock wave. Finally, a continuous RDW was obtained in the combustor. During the initiation stage of the RDW, the average peak pressure of the detonation wave was approximately 0.581 MPa, and the fluctuation in the peak pressure was negligible.

The engine was successfully ignited when the total air temperature was 573 K. The initial detonation wave from the predetonator decoupled and formed two fast deflagration waves propagating in opposite directions after entering the combustor. The weak pressure peak of the fast deflagration wave was measured by P_c at approximately 3500.304 ms, as shown in Fig. 6. After approximately 3.904 ms, the fast deflagration wave transformed into a detonation wave. The average peak pressure was approximately 0.411 MPa, and the peak pressure fluctuated sharply. In addition, large-scale decoupling of the detonation wave occurred during the initiation stage. It is inferred that uneven heating of gasoline droplets causes an asymmetrical distribution of the droplet size in space at low temperatures. The spatial inhomogeneity of gasoline vapour concentration led to a significant chemical reactivity difference between gasoline and air mixtures in the local zone. Thus, the peak pressure of the detonation wave fluctuated significantly, and the RDW decoupled and reignited many times.

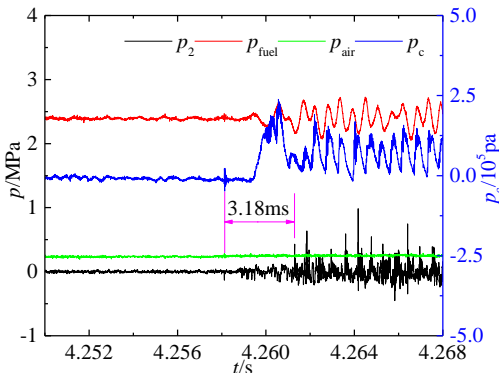


Fig. 7. Initiation stage of RDW in Case #3.

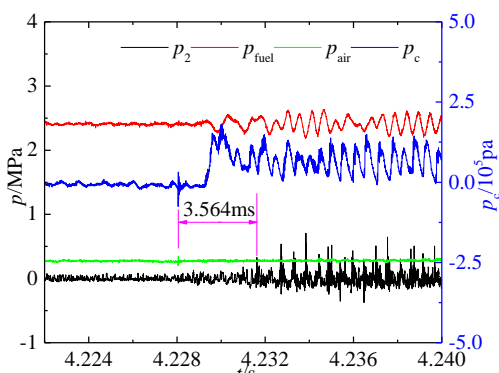


Fig. 8. Initiation stage of RDW in Case #5.

By increasing the total air temperature to 643 K, the time-dependent pressure distribution during the initiation stage of the RDW was obtained, as shown in Fig. 7. Approximately 3.18 ms after the first pressure peak measured by P_c , P_2 detected periodic pressure jump signals, indicating that the RDW propagated continuously in the annular combustor. There was no apparent decoupling of the RDW. The average peak pressure of the RDW was approximately 0.52 MPa, which was higher than that in Case #2, and the fluctuation of the peak pressure was weaker. It is inferred that the spatial distribution uniformity of the gasoline vapour concentration was improved owing to an increase in the total air temperature. With the increase in air temperature, the percentage of active molecules in the gasoline-air mixtures increased, which is conducive to the self-sustained propagation of the detonation wave.

The time-dependent pressure distribution during the RDW initiation stage when the total temperature was increased to 793 K are shown in Fig. 8. The first peak pressure measured by P_c was significantly lower than that in Case #4. After approximately 3.564 ms, P_2 detected the pressure signal of the detonation wave, and the average peak pressure was approximately 0.457 MPa. The fluctuation of the peak pressure was weak, and a multiwave collision phenomenon existed during the initiation stage.

As revealed in Figs. 5–8, the initiation time of the RDW decreased first and then increased with the increase in total air temperature, and reached the minimum value of 2.528 ms at a total air temperature of 713 K. In contrast, the average peak pressure of

the RDW increased first and then decreased with the increase in total air temperature, and reached the maximum value of 0.581 MPa when the total air temperature was 713 K, as shown in Fig. 9. The volume fraction and spatial distribution uniformity of gasoline vapour in the fuel improved with an increase in the total air temperature. Owing to the higher chemical reactivity of gaseous gasoline compared with liquid gasoline, the chemical reaction rate of the reactants was accelerated. The initiation time decreased continuously in the range of 573–713 K with an increase in the total air temperature, and the average peak pressure of the RDW increased. In addition, the ignition temperature of gasoline was 688–803 K. When the total air temperature was 793 K, part of the gasoline and air mixtures burned in deflagration mode ahead of the arrival of the detonation wave, which led to a decrease in the fresh reactant height and gasoline vapour content. Thus, when the total air temperature was increased to 793 K, the initiation time increased, and the average peak pressure of the RDW decreased.

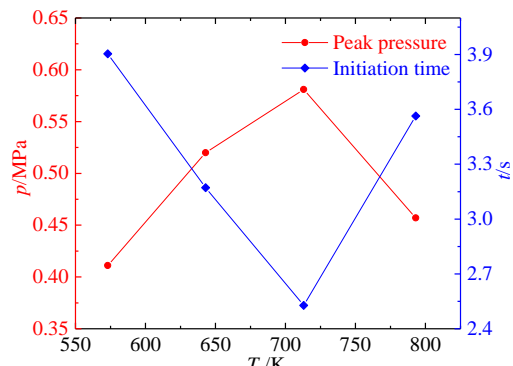


Fig. 9. Initiation time and average peak pressure of RDW with air total temperature.

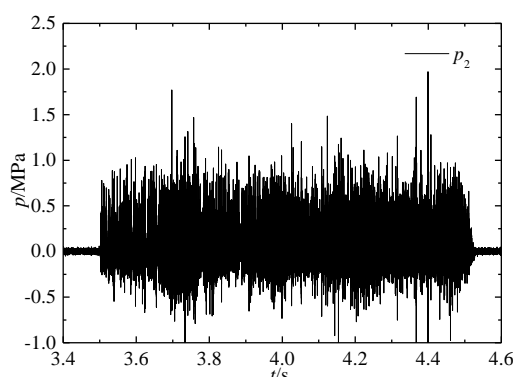


Fig. 10. Global high-frequency pressure signals in Case #2.

3.2 Effect of Total Air Temperature on Propagation Mode

When the total air temperature was 573 K, the propagation mode of the RDW was unstable intermittent detonation, as shown in Case #2 in Table 1. Figure 10 shows the global high-frequency pressure signals measured by P_2 . It was found that

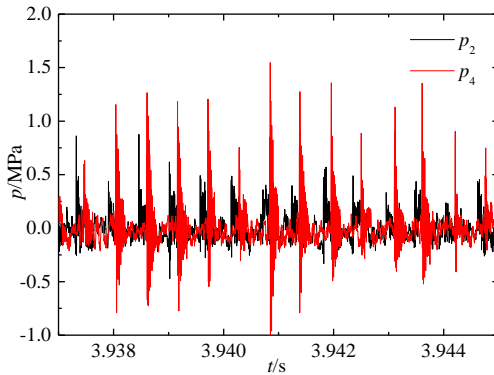


Fig. 11. Local high-frequency pressure signals in Case #2.

the RDW decoupled and reignited many times owing to the uneven spatial distribution of reactant reactivity caused by the low total air temperature during the first half of the combustor operating time. With an increase in the operating time, the combustor wall temperature increased sharply, which promoted the evaporation of gasoline droplets and improved the spatial distribution uniformity of the reactant chemical reactivity. The propagation stability of the RDW was enhanced, and no apparent flameout phenomenon occurred at later operating times. Figure 11 shows the local high-frequency pressure signals measured using P2 and P4. Combined with the phase difference of the high-frequency pressure transducers, it is inferred that a single detonation wave propagates in the annular combustor in the clockwise direction, and the peak pressure of the RDW fluctuates significantly. During the period of 3937.908–3944.764 ms, the reactivity of the reactants near P4 was higher than that at P2. When the RDW propagated to P4, the peak pressure of the detonation wave increased sharply, which is shown as the periodic strong–weak alternation of the peak pressure at P4 and P2.

The propagation mode of the RDW was analysed by increasing the total air temperature to 713 K. Figure 12 shows the local high-frequency pressure signals measured using P2 and P4. The pressure signals oscillated sharply in the cycle, indicating that a continuous rotating detonation wave propagated in the combustor. According to the position distribution of the transducers, the propagation direction of the RDW was clockwise. Owing to the higher total air temperature than that in Case #2, the evaporation rate of gasoline droplets and molecular motion velocity were improved. This improved the spatial distribution uniformity of the chemical reaction reactivity, which is shown as the weaker peak pressure fluctuation of the RDW. In addition, a series of low-peak-pressure oscillations existed after RDWs, as shown in area A in Fig. 12. It is inferred that these low-peak-pressure oscillations were caused by two-phase turbulent combustion. Under the shear force of high total temperature air, light components and heavy components in gasoline droplets break up and evaporate into gasoline vapour. The detonation wave swept the gasoline vapour and air mixtures preferentially. The remaining heavy gasoline components in the region

behind the RDW still burned with air in the deflagration mode. The peak pressure of the two-phase turbulent combustion wave was lower than that of the RDWs.

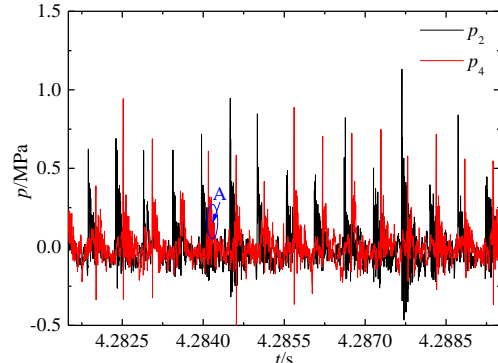


Fig. 12. Local pressure signals in Case #4.

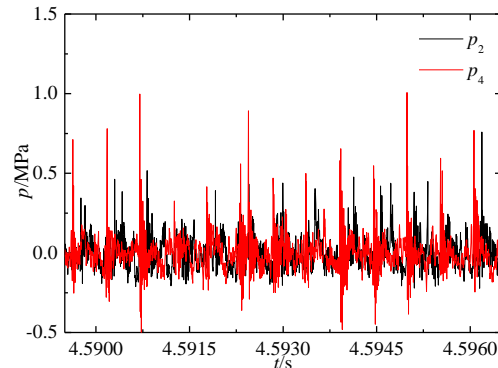


Fig. 13. Local pressure signals in Case #5.

Figure 13 shows the local high-frequency pressure signals measured by P2 and P4 in Case #5. Under this condition, the total air temperature was 793 K, which is close to the upper limit of the gasoline ignition temperature. Based on the high-frequency pressure signals during the test, it was found that the propagation mode of the RDW was a double-wave collision, and the collision point was moving. This may be because of the differences in the local pressure in the combustor and the transmitted shock wave intensity after each collision cycle. This affected the injection state and mixing effect of gasoline and air, resulting in the spatial distribution differences of the fresh reactant height and chemical reactivity. Thus, the collision point changed, as shown in Fig. 13. At approximately 4595.524 ms, the propagation mode of the RDW transformed from a double-wave collision mode to a single-wave mode. This was mainly because of the high pressure at P4 in the previous periods, which inhibited the injection of fresh reactants and led to a low mixture height at P4. When the clockwise transmitted shock wave (viewed from the combustor exit) propagated to P4 at the time, the transmitted shock wave was not enhanced, and it was difficult to develop a new detonation wave. Finally, only one detonation wave propagated counterclockwise in the combustor. With the expansion of detonation products, the local pressure at P4 decreased, and the gasoline and air

injection states recovered. The propagation mode of the RDW transformed from a single-wave to a double-wave collision mode.

With an increase in the total air temperature from 573 K to 713 K, the volume fraction of gasoline vapour in the fuel and the average molecular energy of gasoline-air mixtures increased. This improved the reactivity of the reactants and enhances the ability to resist the influence of lateral expansion. The propagation mode of the detonation wave changed from intermittent detonation to relatively stable single-wave detonation. When the total air temperature was 793 K, part of the gasoline-air mixtures burned ahead of time in the deflagration mode. The increase in local hot spots promoted the formation of a new detonation wave. The propagation mode of the RDW was a mixed mode of double-wave collision and single wave, and the peak pressure of the RDW was lower than that in Case #4.

3.3 Effect of Total Air Temperature on Propagation Characteristics

The peak pressure fluctuation and propagation frequency of the RDW were analysed to investigate its propagation characteristics. Figure 14(a)–(d) show the time-dependent peak pressure distributions of the RDW during the relatively stable stage in Case #2–5, respectively. It can be seen that the RDW propagated in a single wave mode at a total air temperature of 573–713 K. When the total air temperature was 793 K, the propagation mode of the detonation wave was a mixed mode of double-wave collision and single wave. The average peak pressure of the RDW and its standard deviation at different total air temperatures were calculated to evaluate the peak pressure stability of the detonation wave. The results show that the average peak pressure of the RDW first increased and then decreased with an increase in the total air temperature, reaching a maximum value of 0.636 MPa at a total air temperature of 713 K, as shown in Fig. 15. In the pressure characteristics research of hydrogen-fuelled RDW, the peak pressure decreased with an increase in the total air temperature (Yang 2017), which is different from that of gasoline-fuelled RDW. The detonation combustion of gasoline involves the breakup and evaporation of gasoline droplets. With an increase in the total air temperature, the volume fraction of gasoline vapour in the fuel increased. The average molecular energy and molecular motion velocity were enhanced, which improved the chemical reaction rate and energy release rate of the gasoline vapour and air mixtures. However, the air sound velocity increased with an increase in the total air temperature, increasing the fresh reactant height. Thus, when the total air temperature increased from 573 K to 713 K, the average peak pressure of the RDW increased. When the total air temperature was increased to 793 K, the gasoline-air mixtures burned ahead of time in the deflagration mode. The propagation mode of the RDW was a double-wave collision, which led to a decrease in the fresh reactant height and detonation wave peak pressure. In addition, the standard deviation of the detonation wave peak pressure decreased with an increase in the

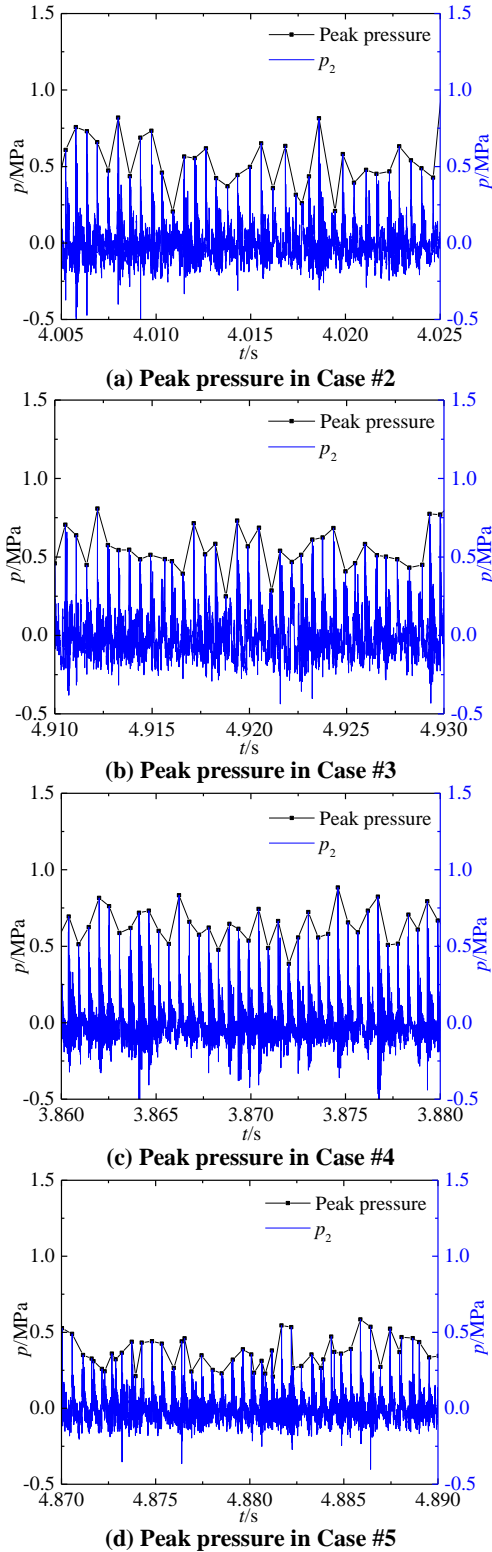


Fig. 14. Pressure distribution of RDW during relatively stable stage.

total air temperature. This indicated that the peak pressure stability of the detonation wave increased gradually. It is inferred that the chemical reactivity of gasoline vapour is higher than that of liquid gasoline. With an increase in the total air temperature, the volume fraction of gasoline vapour in the fuel and its spatial distribution uniformity

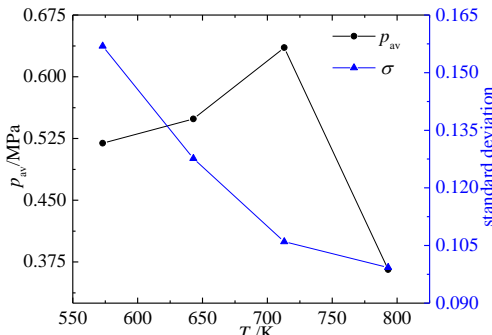


Fig. 15. Average peak pressure and corresponding standard deviation with total air temperature.

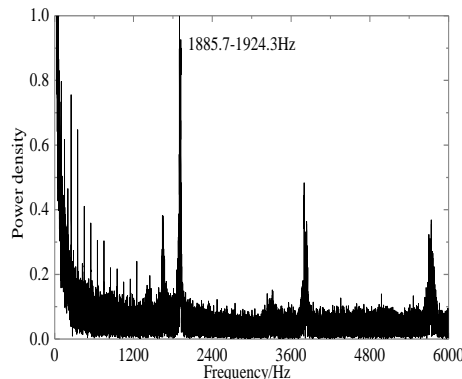


Fig. 16. FFT results in Case #4.

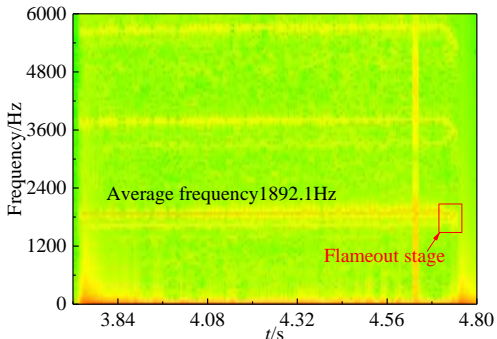


Fig. 17. STFT result in Case #4.

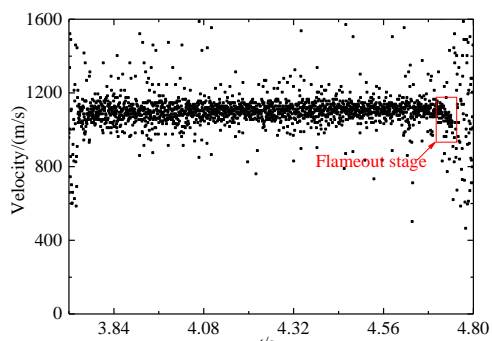


Fig. 18. Propagation velocity of RDW in Case #4.

increased, resulting in an improvement in the detonation wave pressure stability.

Considering the peak pressure and propagation stability of the RDW, frequency domain and time

domain analyses of high-frequency pressure signals measured by P2 in Case #4 were carried out. The distribution of the power spectral density with frequency obtained by the fast Fourier transform (FFT) is shown in Fig. 16. The FFT results show that the dominant frequency of RDW oscillated in the range of 1885.7–1924.3 Hz, and the maximum dominant frequency was approximately 1900.9 Hz. The short-time Fourier transform (STFT) results show the time-frequency characteristics of high-frequency pressure signals, as shown in Fig. 17. Notably, the propagation frequency of the RDW was relatively stable before 4327.938 ms, and no apparent frequency oscillation occurred. The average propagation frequency of the detonation wave was approximately 1892.1 Hz. During the later combustor operating time, slight oscillations occurred in the propagation frequency of the RDW. It is inferred that the combustor wall temperature increases with an increase in the combustor operating time, which increases the percentage of active molecules in the fuel and the reactivity of the gasoline-air mixture. Thus, there was a slight increase in the detonation wave propagation frequency. However, the combustor operating time was short, and the frequency fluctuations were weak. When the solenoid valve of the gasoline pipeline is closed, the equivalence ratio of gasoline-air mixtures before RDW decreased, leading to a decrease in the detonation wave propagation velocity and propagation frequency, as shown in the flameout stage in Fig. 17 and Fig. 18.

The pressure peak time of the high-frequency pressure signals measured by P2 was recorded, and the propagation velocity of the RDW in each propagation cycle was calculated. The distribution of instantaneous propagation velocity with time is shown in Fig. 18. The propagation velocity of RDW fluctuated between 1054.6 and 1155.9 m/s, and the average propagation frequency was 1891.5 Hz based on the average propagation velocity, which is consistent with the FFT and STFT results. Under this condition, the CJ detonation velocity was 1817.2 m/s, and there was a heavy velocity deficit in the propagation velocity of the RDW.

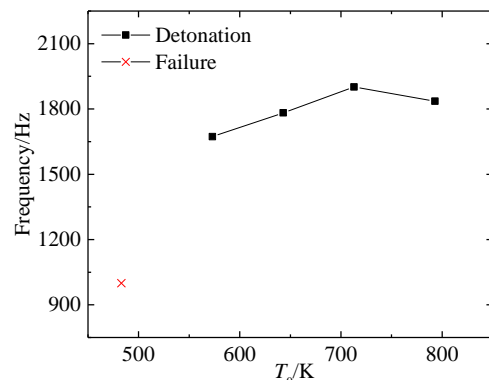


Fig. 19. Propagation frequency distribution with total air temperature.

Figure 19 shows the variation trend of the propagation frequency with total air temperature. Noticeably, the detonation initiation failed when the

total air temperature was 483 K. Increasing the total air temperature to 573 K caused the detonation initiation to succeed and propagate in the single-wave mode with a propagation frequency of 1672.4 Hz. With an increase in the total air temperature, the volume fraction of gasoline vapour in the fuel increased, and the average molecular energy and molecular motion velocity increased. This resulted in an improvement in the mixing effect and spatial distribution uniformity of the reactants, which is shown as a continuous increase in the detonation wave propagation frequency. When the total air temperature was 713 K, the maximum value of the propagation frequency was 1900.9 Hz. There was a heavy energy loss owing to the deflagration combustion of gasoline and air when the total air temperature was increased to 793 K; thus, the propagation frequency of the RDW decreased.

3.4 Effect of Equivalence Ratio on Combustor Working Characteristics

Based on the experimental results in Fig. 19, the effect of the equivalence ratio on the working characteristics of the two-phase RDE was studied under a wide range of operating conditions by changing the gasoline mass flow rate at a total air temperature of 713 K. Figure 20 shows the variation in the detonation wave propagation mode with the increase in equivalence ratio. It can be seen that the propagation stability of the RDW was poor under the condition of low equivalence ratios. The propagation mode of the detonation wave was sporadic detonation or intermittent detonation, as shown in Fig. 21. When the equivalence ratio was 0.66, the detonation wave decoupled and reignited several times during the propagation process. When the equivalence ratio was reduced to 0.61, only sporadic pressure signals of the detonation wave appeared during the entire test. When the equivalence ratio was reduced to 0.53, detonation initiation failed. This is mainly because the gasoline mass flow rate is relatively low under low equivalence ratios, resulting in low gasoline vapour concentration in combustible reactants. Severe spatial distribution inhomogeneity of the equivalence ratio is shown as the poor propagation stability of the RDW. When the equivalence ratio was between 0.79 and 0.97, the propagation mode of the RDW was a mixed mode of double wave collision and single wave. The propagation mode transformed into a single-wave mode by further increasing the equivalence ratio to 1.06–1.25. The reason for the mode transition may be that one key condition for maintaining double-wave collision is the rapid establishment of a fresh reactant layer height. Under the condition of high equivalence ratios, the peak pressure of the RDW increased, which led to a longer choked time for reactant injection behind the detonation wave. The rapid establishment of a fresh reactant layer was inhibited; thus, the propagation mode of the detonation wave changed from a mixed mode to a single-wave mode.

Figure 22 shows the variation trend of the average absolute pressure in the combustor and average propagation frequency of the RDW with an increase

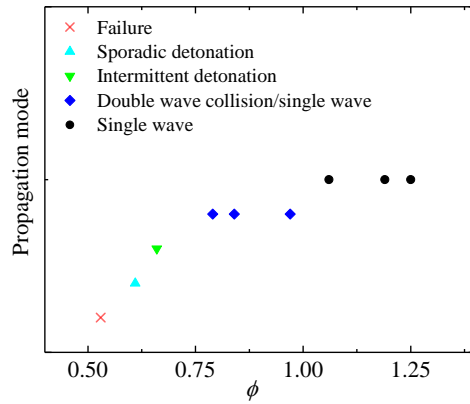
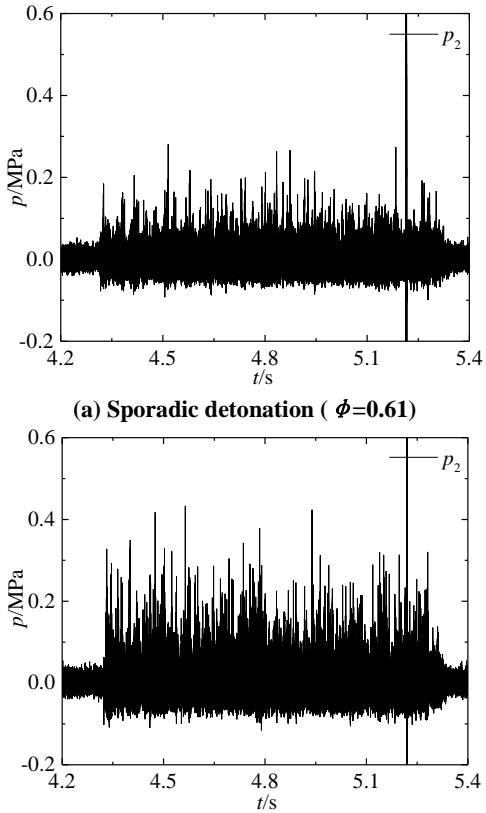


Fig. 20. Propagation mode under the condition of different equivalence ratios.



(a) Sporadic detonation ($\phi=0.61$)
(b) Intermittent detonation ($\phi=0.66$)

Fig. 21. Unstable propagation mode of RDW under the condition of low equivalence ratios.

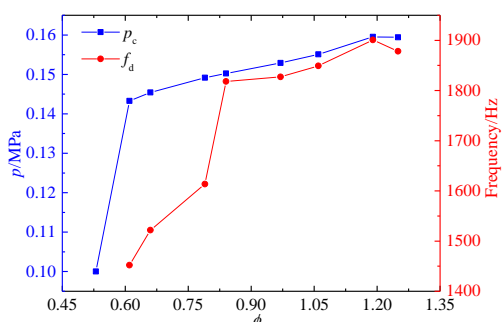


Fig. 22. Distribution of absolute pressure in the combustor and propagation frequency of RDW with equivalence ratio.

in the equivalence ratio. Noticeably, the combustor pressure and propagation frequency first increased and then decreased with an increase in the equivalence ratio. It is inferred that the spatial distribution uniformity of gasoline vapour concentration and the mixing effect of reactants are improved owing to the increase in the gasoline mass flow rate. However, when the equivalence ratio was increased to 1.25, the oxygen concentration in the gasoline-air mixtures decreased, and the reactivity of the reactants decreased. The maximum values were obtained at an equivalence ratio of 1.19, which is a slightly rich fuel condition. The reason may be as follows: on the one hand, under the shear force of high total temperature air, the remaining heavy components in gasoline still existed in the form of small droplets and did not participate in the detonation combustion; on the other hand, owing to the radial injection of air, the collision and aggregation effect of axially injected atomised gasoline particles was intensified, and some gasoline particles adsorbed on the combustor wall, resulting in an actual reactant equivalence ratio lower than the experimental set value. Therefore, when the equivalence ratio was 1.19, the actual reactant equivalence ratio was closer to the ideal chemical equivalence ratio.

3.5 Long-Duration Test

A long-duration test was performed to verify the continuous working feasibility of a two-phase RDE operating with high total temperature air and gasoline. Temperature drift occurs in high-frequency pressure signals owing to the influence of high-temperature detonation products. When the test time was too long, the measured voltage signals exceeded the lower limit of the pressure transducers, and the pressure transducers suffered irreversible damage from shock waves and high-temperature detonation products. Therefore, diffused silicon pressure transmitters with fast response times were utilised to measure the pressure in the combustor and gasoline plenum instead of piezoelectric pressure transducers in the long-duration test. The test duration was set to

3 s to avoid heavy damage to the diffused silicon pressure transmitters and the combustor wall.

Figure 23 shows the test results for Case #10. The equivalence ratio of the propellants was 0.84, and the total air temperature was 713 K. The propagation mode of the RDW was a mixed mode of double-wave collision and single wave. With the continuous propagation of the RDW, the average pressure in the combustor and gasoline plenum oscillated at a high frequency, and there was a large increase in the average pressure measured in the combustor. The dominant frequency of the RDW obtained from the FFT result was 1818.21 Hz. The inset in Fig. 23 shows that the oscillation frequency of the pressure in the gasoline plenum was consistent with the propagation frequency of the RDW. When the detonation wave reached the circumferential position of P_{fuel} , the local pressure at the nozzle exit increased, which led to a decrease in the injection speed and an increase in the pressure in the gasoline plenum. With the forward propagation of the detonation wave, the local pressure decreased owing to the expansion of the detonation products, and the injection speed of gasoline gradually recovered; thus, the pressure in the gasoline plenum decreased. A dynamic balance was established between the pressure in the combustor and the gasoline plenum.

Case #14 was the corresponding long-duration test for Case #10. The test results are shown in Fig. 24. During the entire combustor operating time, high-frequency pressure oscillations were observed in the pressure measured in the gasoline plenum and combustor. There was a noticeable pressure rise in the average combustor pressure, which is consistent with that in Case #10. The first pressure oscillation signal was detected at 4370.46 ms in the combustor. At approximately 7459.45 ms, the time-average pressure amplitude decreased and finally decayed to the ambient pressure at 7501.92 ms. The combustor operating time was approximately 3131.46 ms, and the average absolute pressure in the combustor was approximately 0.151 MPa. Figure 25 shows the STFT results of the pressure signals measured in the

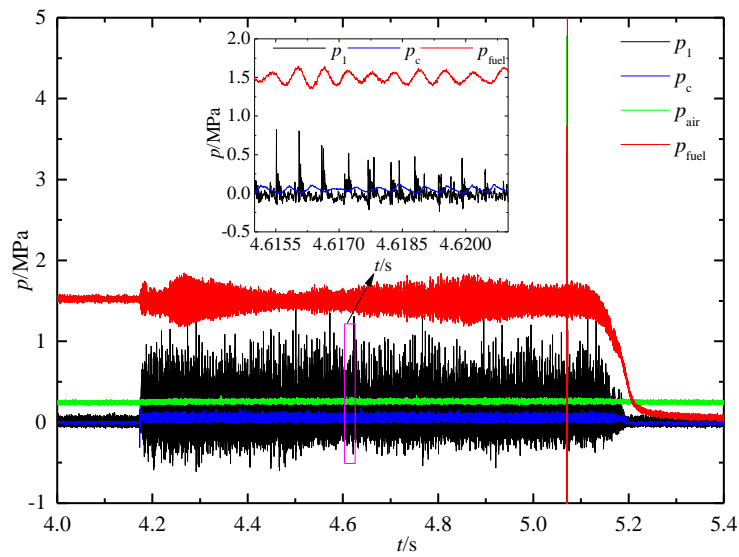


Fig. 23. Global pressure distribution and local pressure oscillation in the gasoline plenum in Case #10.

gasoline plenum, where the average propagation frequency of the RDW was approximately 1922.3 Hz, which was slightly higher than that in Case #10. It is inferred that a rapid rise in the combustor wall temperature accelerates the evaporation of gasoline droplets and improves the mixing effect and average molecular energy of the reactants. Thus, the propagation frequency of the RDW increased with combustor operating time.

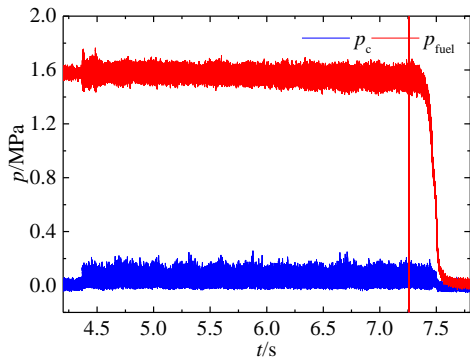


Fig. 24. Average pressure in the gasoline plenum and combustor in Case #14.

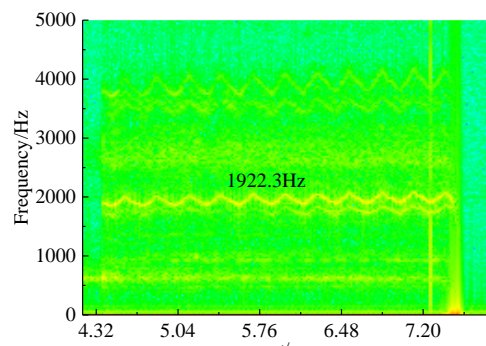


Fig. 25. STFT result in the gasoline plenum in Case #14.

4. CONCLUSIONS

A series of experimental tests were performed to investigate the effect of the total air temperature on the initiation characteristics, propagation mode, and propagation characteristics of two-phase RDW with gasoline-air mixtures. Three detonation propagation modes (intermittent detonation, single wave, coexistence of double wave collision, and single wave) were obtained when the total air temperature increased from 573 K to 793 K. When the total air temperature was reduced to 483 K, detonation initiation failed.

It was found that the initiation time first decreased and then increased with an increase in the total air temperature, and a minimum value of 2.528 ms was reached at a total air temperature of 713 K. In contrast, the average peak pressure of the RDW during the initiation stage reached a maximum value of 0.581 MPa when the total air temperature was 713 K. In addition, the peak pressure stability of the RDW intensified with an increase in total air temperature. The average peak pressure and propagation frequency of the RDW first increased

and then decreased with increasing total air temperature. The maximum values appeared around a total air temperature of 713 K. The corresponding average propagation velocity was 1110.8 m/s. A heavy velocity deficit existed during the propagation of the detonation wave.

The effect of the equivalence ratio on the working characteristics of the RDE was studied, based on the experimental results, at a total air temperature of 713 K. Experimental results show that four propagation modes (sporadic detonation, intermittent detonation, coexistence of double wave collision and single wave, and single wave) of RDW could be obtained by varying the equivalence ratio. When the equivalence ratio was 0.52, the detonation initiation failed. In addition, the average absolute pressure in the combustor and propagation frequency of the RDW first increased and then decreased with an increase in the equivalence ratio. The maximum values appeared at an equivalence ratio of 1.19.

Moreover, a long-duration test was performed to verify the feasibility of continuous working in a two-phase RDE operating with high total temperature air. The results showed that the continuous propagation of the RDW was realised in the combustor, and the two-phase RDE worked for 3131.46 ms. It was found that the propagation frequency of the RDW increased with the working time owing to the rapid rise of the combustor wall temperature.

ACKNOWLEDGEMENTS

This work was supported by the National Natural Science Foundation of China (12072163, 52106161, 11802134), National Defense Science and Technology Key Laboratory Foundation (HTKJ2020KL011004-1), and Chinese Postdoctoral Science Foundation (2020M681616).

REFERENCES

- Anand, V., A. S. George, R. Driscoll and E. Gutmark (2016). Investigation of rotating detonation combustor operation with H₂-Air mixtures. *International Journal of Hydrogen Energy* 41(2), 1281-1292.
- Bykovskii, F. A., S. A. Zhdan and E. F. Vedernikov (2014). Initiation of detonation of fuel-air mixtures in a flow-type annular combustor. *Combustion Explosion and Shock Waves* 50(2), 214-222.
- Bykovskii, F. A. and E. F. Vedernikov (2003). Continuous detonation of a subsonic flow of a propellant. *Combustion Explosion and Shock Waves* 39(3), 323-334.
- Bykovskii, F. A., S. A. Zhdan and E. F. Vedernikov (2006a). Continuous spin detonation of fuel-air mixtures. *Combustion Explosion and Shock Waves* 42(4), 463-471.
- Bykovskii, F. A., S. A. Zhdan and E. F. Vedernikov (2006b). Continuous spin detonations. *Journal of Propulsion and Power* 22(6), 1204-1216.

- Bykovskii, F. A., S. A. Zhdan and E. F. Vedernikov (2016). Continuous spin detonation of a heterogeneous kerosene-air mixture with addition of hydrogen. *Combustion Explosion and Shock Waves* 52(3), 371-373.
- Bykovskii, F. A., S. A. Zhdan and E. F. Vedernikov (2019). Continuous detonation of the liquid kerosene-air mixture with addition of hydrogen or syngas. *Combustion Explosion and Shock Waves* 55(5), 589-598.
- Bykovskii, F. A., V. V. Mitrofanov and E. F. Vedernikov (1997). Continuous detonation combustion of fuel-air mixtures. *Combustion Explosion and Shock Waves* 33(3), 344-353.
- Deng, L., H. Ma, C. Xu, C. Zhou and X. Liu (2017). Investigation on the propagation process of rotating detonation wave. *Acta Astronautica* 139(Oct.), 278-287.
- Fotia, M. L., J. Hoke and F. Schauer (2018). Study of the ignition process in a laboratory scale rotating detonation engine. *Experimental Thermal and Fluid Science*, 94, 345-354.
- Frolov, S. M., V. I. Zvegintsev, V. S. Ivanov, V. S. Aksenov, I. O. Shamshin and D. A. Vnuchkov (2018). Hydrogen-fueled detonation ramjet model: Wind tunnel tests at approach air stream Mach number 5.7 and stagnation temperature 1500K. *International Journal of Hydrogen Energy* 43, 7515-7524.
- Frolov, S. M., V. S. Aksenov, V. S. Ivanov and I. O. Shamshin (2015). Large-scale hydrogen-air continuous detonation combustor. *International Journal of Hydrogen Energy* 40(3), 1616-1623.
- Frolov, S. M., V. S. Aksenov, V. S. Ivanov and I. O. Shamshin (2017). Continuous detonation combustion of ternary "hydrogen-liquid propane-air" mixture in annular combustor. *International Journal of Hydrogen Energy* 42(26), 16808-16820.
- Ge, G., L. Deng, H. Ma, X. Liu, L. Jin and C. Zhou (2019). Effect of blockage ratio on the existence of multiple waves in rotating detonation engine. *Acta Astronautica* 164(Nov.), 230-240.
- Kindracki, J. (2012). Experimental studies of kerosene injection into a model of a detonation chamber. *Journal of Power Technologies* 92(2), 80-89.
- Kindracki, J. (2014). Study of detonation initiation in kerosene-oxidizer mixtures in short tubes. *Shock Waves* 24(6), 603-618.
- Kindracki, J. (2015). Experimental research on rotating detonation in liquid fuel-gaseous air mixtures. *Aerospace Science and Technology* 43, 445-453.
- Li, B., Z. Wang, G. Xu, C. Weng and F. Zhao (2020). Experimental research on initiation and propagation characteristics of kerosene fuel rotating detonation wave. *Acta Armamentarii* 41(7), 1339-1346.
- Liu, S., W. Liu, Z. Lin and W. Lin (2015). Experimental research on the propagation characteristics of continuous rotating detonation wave near the operating boundary. *Combustion Science and Technology* 187(10-12), 1790-1804.
- Peng, L., D. Wang, X. Wu, H. Ma and C. Yang (2015). Ignition experiment with automotive spark on rotating detonation engine. *International Journal of Hydrogen Energy* 40(26), 8465-8474.
- Rankin, B. A., D. R. Richardson, A. W. Caswell, A. G. Naples, J. L. Hoke and F. R. Schauer (2017). Chemiluminescence imaging of an optically accessible non-premixed rotating detonation engine. *Combustion and Flame* 176, 12-22.
- Wang, C., W. Liu, S. Liu, L. Jiang and Z. Lin (2015). Experimental verification of air-breathing continuous rotating detonation fueled by hydrogen. *International Journal of Hydrogen Energy* 40(30), 9530-9538.
- Wang, D., J. Zhou and Z. Lin (2017). Experimental investigation on operation characteristics of two-phase continuous rotating detonation combustor fueled by kerosene. *Journal of Propulsion Technology* 38(2), 471-480.
- Wolanski, P. (2013). Detonative propulsion. *Proceedings of the Combustion Institute* 34(1), 125-158.
- Xia, Z., H. Ma, C. Liu, C. Zhuo and C. Zhou (2019). Experimental investigation on the propagation mode of rotating detonation wave in plane-radial combustor. *Experimental Thermal and Fluid Science* 103(May), 364-376.
- Xie, Q., H. Wen, W. Li, Z. Ji, B. Wang and P. Wolanski (2018). Analysis of operating diagram for H₂/Air rotating detonation combustors under lean fuel condition. *Energy* 151(May15), 408-419.
- Yang, C. (2017). *Investigation on the initiation and propagation characteristics of rotating detonation Wave*, PhD Thesis, Nanjing University of Science and Technology, Nanjing, China.
- Yang, C., X. Wu, H. Ma, L. Peng and J. Gao (2016). Experimental research on initiation characteristics of a rotating detonation engine. *Experimental Thermal and Fluid Science*, 71, 154-163.
- Zheng, Q., B. Li, C. Weng and Q. Bai (2017). Thrust measurement of liquid-fueled rotating detonation engine under two-wave collision mode. *Acta Armamentarii* 38(4), 679-689.
- Zheng, Q., C. Weng and Q. Bai (2015). Experimental study on effects of equivalence ratio on detonation characteristics of liquid-fueled rotating detonation engine. *Journal of Propulsion Technology* 36(6), 947-952.